View metadata, citation and similar papers at core.ac.uk

brought to you by CORE

provided by IUPUIScholarWorks

ACCEPTED MANUSCRIPT

R125H, W240S, C386R, and V507I SLC4A11 Mutations Associated with Corneal Endothelial Dystrophy Affect the Transporter Function but not Trafficking in PS120 cells

Shimin Li[2], Karmjot Singh Hundal[1], Xingjuan Chen[1], Moonjung Choi[2], Diego G. Ogando[2], Alexander G. Obukhov[1], Joseph A. Bonanno[2]

[1]Department of Cellular & Integrative Physiology – IU School of Medicine, Indianapolis, Indiana

[2]School of Optometry, Indiana University Bloomington, Bloomington, Indiana

Corresponding Authors:
Joseph A. Bonanno
jbonanno@indiana.edu

and

Alexander G. Obukhov
aobukhov@iu.edu

ACCEPTED MANUSCRIPT

This is the author's manuscript of the article published in final edited form as:

Li, S., Hundal, K. S., Chen, X., Choi, M., Ogando, D. G., Obukhov, A. G., & Bonanno, J. A. (2019). R125H, W240S, C386R, and V507I SLC4A11 mutations associated with corneal endothelial dystrophy affect the transporter function but not trafficking in PS120 cells. Experimental Eye Research, 180, 86–91. https://doi.org/10.1016/j.exer.2018.12.003

ACCEPTED MANUSCRIPT

Abstract

SLC4A11 mutations are associated with Fuchs' endothelial corneal dystrophy (FECD), congenital hereditary endothelial dystrophy (CHED) and Harboyan syndrome (endothelial dystrophy with auditory deficiency). Mice with genetically ablated *Slc4a11* recapitulate CHED, exhibiting significant corneal edema and altered endothelial morphology. We recently demonstrated that SLC4A11 functions as an NH_3 sensitive, electrogenic H^+ transporter. Here, we investigated the properties of five clinically relevant *SLC4A11* mutants: R125H, W240S, C386R, V507I and N693A, relative to wild type, expressed in a PS120 fibroblast cell line. The effect of these mutations on the NH_4Cl-dependent transporter activity was investigated by intracellular pH and electrophysiology measurements. Relative to plasma membrane expression of Na-K ATPase, there were no significant differences in plasma membrane SLC4A11 expression among each mutant and wild type. All mutants revealed a marked decrease in acidification in response to NH_4Cl when compared to wild type, indicating a decreased H^+ permeability in mutants. All mutants exhibited significantly reduced H^+ currents at negative holding potentials as compared to wild type. Uniquely, the C386R and W240S mutants exhibited a different inward current profile upon NH_4Cl challenges, suggesting an altered transport mode. Thus, our data suggest that these SLC4A11 mutants, rather than having impaired protein trafficking, show altered H^+ flux properties.

Key Words: SLC4A11; intracellular pH; Ammonia; proton flux; patch clamp

ACCEPTED MANUSCRIPT

ACCEPTED MANUSCRIPT

SLC4A11 has been identified to be a member of Solute Carrier 4 (SLC4) family of bicarbonate transporters. It was initially reported to function as an electrogenic membrane transporter for Na^+-coupled borate (Park, Li et al. 2004), however recent studies indicate that human SLC4A11 does not transport bicarbonate or borate (Jalimarada, Ogando et al. 2013; Kao, Azimov et al. 2016; Loganathan, Schneider et al. 2016; Ogando, Jalimarada et al. 2013). We have provided evidence that SLC4A11 has H^+ permeability that is activated by ammonia and is directly proportional to $[NH_3]_o$ not $[NH_4^+]_o$, and is relatively unaffected by removal of Na^+, K^+, or Cl^- (Zhang, Ogando et al. 2015).

Several mutations in SLC4A11 have been reported to be associated with Fuchs' endothelial corneal dystrophy (FECD), congenital hereditary endothelial dystrophy (CHED2) and Harboyan syndrome (endothelial dystrophy with auditory deficiency). Specifically, the C386R and R125H mutants of SLC4A11 are found in patients with autosomal recessive Congenital Hereditary Endothelial Dystrophy, whereas the V507I and W240S mutants of SLC4A11 are linked to Fuchs endothelial corneal dystrophy (Ramprasad, Ebenezer et al. 2007; Riazuddin, Vithana et al. 2010; Vithana, Morgan et al. 2006). Corneal endothelial dystrophy and the associated dysfunction of the corneal endothelial cells may lead to corneal edema and blindness in humans that currently can only be treated by corneal transplant.

The R125H and W240S mutations are both localized in the SLC4A11 N-terminal cytoplasmic domain. C386R and V507I mutations are localized in the 1^{st} or 5^{th} transmembrane domains respectively, whereas N639A is located in extracellular loop 4. It has been reported that some SLC4A11 mutations may cause dysfunction of the protein and/or reduced trafficking to the plasma membrane (Alka and Casey 2018; Alka and Casey 2018; Chiu, Mandziuk et al. 2015; Vilas, Loganathan et al. 2013; Vilas, Loganathan et al. 2012; Vithana, Morgan et al. 2008). Function of mutants has been tested by measuring changes in water flux (Alka and Casey 2018; Chiu, Mandziuk et al. 2015; Vilas, Loganathan et al. 2013)**,** which is small relative to aquaporins, in HEK cells or Xenopus oocytes and electrophysiologically using the R109H mouse mutant in Xenopus oocytes (Myers, Marshall et al. 2016).

In this study, we stably expressed the five human SLC4A11 mutants (R125H, W240S, C386R, V507I and N693A) representing two N-terminal, two transmembrane and one extracellular loop mutants, respectively. The R125H was included as a potentially dysfunctional mutant (Vilas, Loganathan et al. 2013). The hamster fibroblast (PS120) cell line that lacks the Na^+- H^+ exchanger (NHE) was used for transfection. This cell line is used because NHE complicates the investigation of proton fluxes via SLC4A11 (Barriere, Poujeol et al. 2001; Ogando, Jalimarada et al. 2013). We investigated the effect of these mutations on trafficking by plasma membrane protein isolation with reference to the major plasma membrane Na-K-ATPase and functional properties of the SLC4A11 by patch-clamp electrophysiology.

Human *SLC4A11* cDNA was cloned in frame with the hemagglutinin epitope (HA)-tag and was inserted into the phCMV vector. Five single amino acid changes were individually made using the QuikChange Lightning Site-Directed Mutagenesis Kit (Agilent Technologies, CA). Mutated SLC4A11 variants are referred to as R125H, W240S, C386R, V507I, and N639A respectively. To generate these mutants, the following nucleotide changes were made: G374A, G719C, T1157C, G1519A, and AA(1915, 1916)GC, respectively. All mutations were confirmed by DNA sequencing at ACGT, Inc. (Wheeling, IL). Primer sequences used for generating mutations are provided in Table 1. The nucleotides and positions of the mutations are indicated.

Hamster fibroblast (PS120) cells were cultured in DMEM supplemented with 5% fetal bovine serum, and transfected with the *SLC4A11* plasmids using Lipofectamine 3000 (Invitrogen). The cells, which were stably expressing the *SLC4A11* mutants, were selected by Geneticin at 1 mg/ ml in culture medium. The details of the transfection procedure are described elsewhere (Ogando, Jalimarada et al. 2013). PS120 cells stably expressing wild-type *SLC4A11* plasmid (WT) or the empty vector plasmid (EV) were used as controls.

PS120 cell surface proteins were linked to sulfo-NHS-SS-Biotin (Pierce, Rockford, IL) according to the manufacturer's instructions. In brief, transfected PS120 cells grown in two T-75 flasks were incubated with sulfo-NHS-SS-biotin (0.25 mg/ml) at 10 ml/flask for 30 min at 4°C. The cells were washed 3 times with ice-cold PBS and then lysed in 500 µl of lysis buffer [5 mM EDTA, 150 mM NaCl, 1% (vol/vol) Igepal, 0.5% (wt/vol) sodium deoxycholate, 10 mM Tris·HCl, pH 7.5 and protease inhibitors]. The lysate was sonicated at

low power on ice. After a 10-min centrifugation (10,000 *g* at 4°C), the supernatant was collected and incubated with 500 µl of NeutrAvidin Agarose for 1 h with rocking at room temperature. The resin was collected by centrifugation at 1,000 *g* and washed three times with the wash buffer provided with the kit. The supernatant and wash, representing the non-membrane fraction, were collected and saved. Finally the bound proteins were eluted with 400 µl of 2 × SDS sample buffer.

Both fractions (20 µg per lane) were resolved on SDS-PAGE gels. The biotinylated SLC4A11 protein was detected using the anti-HA antibody (Covance Inc. Alice, TX). A plasma membrane protein, Na^+/K^+-ATPase, was used as internal control to normalize the SLC4A11 protein amount in the tested lysate samples. The anti (α-1 subunit) Na^+/K^+-ATPase antibody was from Cell Signaling (#3010). Both membrane and non-membrane fractions were probed for Endoplasmin (GRP94, Bio-Rad #VPA00059), an ER resident protein, and for GAPDH in order to validate the biotinylation procedure. Blot densitometry analysis was performed using the software "Image Lab 6.0" (BIO-RAD).

To measure intracellular pH (pHi), PS120 cells that had been transfected with SLC4A11 constructs were grown on poly-lysine coated coverslips. At about 80% confluence, cells were loaded for 30 minutes at room temperature with a pH sensitive fluorescent dye of 2′,7′-bis-(2-carboxyethyl)-5-(6)-carboxyfluorescein acetoxymethyl ester (BCECF AM, 10 µM, Invitrogen, CA), which was diluted from a 10 mM DMSO stock in a bicarbonate-free buffer (BF Ringer) of the following composition in mM: 105 NaCl, 10 NMDG-Cl, 2 KCl, 0.61 $MgCl_2$, 1 K_2HPO_4, 28.5 Na^+-Gluconate, 1.4 Ca^{2+}-Gluconate, and 10 HEPES. The coverslip was washed for 30 minutes in fresh BF ringer and then mounted in a custom-designed perfusion chamber. BF Ringer was used as the standard bathing solution (pH 7.5 and osmolality 295). The NH_4Cl perfusion solution was prepared by substituting 10 mM NMDG-Cl with 10 mM NH_4Cl in BF Ringer. The perfusion chamber was maintained at 37 °C using a circulating water bath. The perfusion flow rate was kept to ~0.5 ml/min by gravity. Perfusion of NH_4Cl-BF Ringer was conducted for 5 minutes in all experiments. BCECF fluorescence (Ex 495 and 440nm, Em 520-550nm) was captured using an inverted microscope (Eclipse TE200, Nikon, Japan) equipped with the oil-immersion 40x objective. The fluorescence was recorded and analyzed using Felix 32 Software. The

fluorescence emission ratio (Ex_{495}/Ex_{440}) was obtained at 1 Hz and converted to pH via calibration with high-K^+-nigericin (26 µM) in Ringer (Ogando, Jalimarada et al. 2013). All rates of pHi change ($\Delta pHi/\Delta t$) were calculated from the initial 20 seconds following a perfusion change.

The whole-cell patch clamp technique was used to measure NH_4Cl-induced currents through SLC4A11 and mutants as described elsewhere (Zhang, Ogando et al. 2015). Briefly, whole cell currents were amplified using an Axopatch 200B integrating patch-clamp amplifier and digitized using a Digidata 1400 analog-to-digital converter (Molecular Devices, CA). Currents were filtered at 3 kHz using the internal filter of Axopatch 200B and sampled at a rate of 1 kHz. The patch-clamp data were analyzed using the pCLAMP 10 software package. The extracellular solution for electrophysiological recordings contained (in mM): 145 NaCl, 2.5 KCl, 2. $CaCl_2$, 1 $MgCl_2$, 10 HEPES, and 5.5 glucose (pH 7.5 or 8.5, adjusted with NaOH). The pipette solution contained in mM: 125 $CsMeSO_3$, 3.77 $CaCl_2$, 2 $MgCl_2$, 10 EGTA (100 nM free Ca^{2+}), and 10 HEPES (pH 7.2 adjusted with Trizma base). The 10 mM NH_4Cl was always made fresh before the experiments began. The current density (pA/pF) was calculated by dividing the current amplitude by the cell capacitance. All salts were purchased from Sigma-Aldrich. Data were analyzed by one-way ANOVA test. They are shown as mean values $\pm$ standard deviation. $P \leq 0.05$ was considered significant.

Figure 1A shows a representative blot of plasma membrane SLC4A11 expression referenced to Na^+/K^+ ATPase in the biotinylated fraction. Figure 1B shows the summary results from three experiments. The ratio of biotinylated-SLC4A11 to biotinylated-Na^+/K^+ ATPase in Wild Type transfected cells was 0.9. The ratio in the five mutants was not significantly different indicating that those mutants were able to traffic to the plasma membrane. The membrane biotinylation and isolation procedure was validated by probing biotinylated (membrane) and non-biotinylated (cytosolic) fractions for Endoplasmin (GRP94), an ER lumen resident protein and GAPDH, a cytosolic protein. Membrane/cytosolic ratios of GRP94 were approximately 6% and GAPDH less, indicating that there was good separation and little contamination of membrane fractions with ER protein or soluble cytosol.

The ammonia sensitive H^+ flux properties of SLC4A11 were first described using intracellular pH measurements. Figure 1C shows NH_4Cl-induced pHi changes in PS120 cells that had been transfected with WT-SLC4A11, mutant variants, and EV (empty vector). The baseline pHi (Figure 1D) was lowest (7.17 $\pm$ 0.06) in WT-SLC4A11 and highest in EV (7.81 $\pm$ 0.09), consistent with previous findings (Jalimarada, Ogando et al. 2013; Ogando, Jalimarada et al. 2013; Zhang, Ogando et al. 2015), and is attributed to small background electrogenic H^+ influx generated by SLC4A11 (Kao, Azimov et al. 2015; Kao, Azimov et al. 2016; Myers, Marshall et al. 2016; Zhang, Ogando et al. 2015). The five mutants displayed baseline pHi in between WT-SLC4A11 and EV. The pHi increased sharply when cells were exposed to NH_4Cl. Alkalinization rates (ΔpHi/min) were converted to H^+ flux (Figure 1E) (Flux=dpH/dt * β_t), where β_t is intrinsic buffering capacity, which is a function of pHi (β=a*EXP(-b*pHi)+c*EXP(-d*pHi), where a=0.364, b=-0.466, c=7E9, and d=3.04 (buffering data deposited in Menedlay). Cell acidification rates in the presence of NH_4Cl were also converted to H^+ flux (Figure 1F). H^+ fluxes and the total acidification following removal of NH_4Cl (Figure 1G) was WT > C386 > W240 > R125 > V507 > N639 >EV. Total acidification represents the ultimate effect of the NH_4Cl pulse, and it confirmed that SLC4A11 transporter activity and its ability to affect H^+ flux was compromised by the mutations.

We next performed electrophysiological recordings in PS120 cells stably expressing WT-SLC4A11 or mutants. The electrophysiological data revealed that NH_4Cl-induced currents in PS120 cells stably expressing the tested SLC4A11 mutants exhibited significantly reduced average amplitudes compared to that observed in the WT-SLC4A11-PS120 cells (Fig. 2A-G) in both pH 7.4 (Fig. 2I) and pH 8.5 (Fig. 2H) solutions. In pH 8.5 solution, PS120 cells stably expressing R125H (Fig. 2E), V507I (Fig. 2F) or N639R (Fig. 2G) mutants exhibited NH_4Cl-induced inward currents indistinguishable from those observed in PS120 cells stably expressing the empty vector. While all mutant currents were significantly suppressed, the mean amplitude of inward currents in the C386R-SLC4A11-PS120 cells and W240S- SLC4A11-PS120 cells (Fig. 2C and 2D, respectively) was significantly greater than that found in the empty vector at pH 8.5 (Fig. 2H), but not pH 7.5 (Fig 2I). Interestingly, extracellular alkalinization alone (Fig. 2J) induced small inward currents in C386R-

SLC4A11-PS120 cells and W240S-SLC4A11-PS120 cells. Uniquely, no characteristic changes in the current flow direction upon re-addition of pH 7.5 solution after an NH_4Cl extracellular pulse were observed in C386R-SLC4A11-PS120 and W240S-SLC4A11-PS120 cells in sharp contrast to WT-SLC4A11-PS120 cells after an NH_4Cl pulse (Fig. 2K). Alkalinization of the extracellular solution to pH 8.5 did not affect baseline currents in wild type SLC4A11, V507I, R125H or N639A mutant expressing PS120 cells before a second NH_4Cl pulse, but increased the baseline current in C386R-SLC4A11-PS120 and W240S-SLC4A11-PS120 cells (Fig. 2A-G). The NH_4Cl-induced currents recorded at pH 7.4 and pH 8.5 in WT-SLC4A11-PS120 cells were reversing at significantly different membrane potentials of +15.2 ± 2.4 and -17.2 ± 5.2 mV, respectively. In sharp contrast, the reversal potentials of NH_4Cl-induced currents were not significantly different in C386R-SLC4A11-PS120 and W240S-SLC4A11-PS120 cells when the currents were measured under the same conditions (C386R: -7.8 ± 3.5 mV at pH 7.5 and -11.8 ± 6.8 mV at pH 8.5; W240S: -19.1 ± 4.4 mV at pH 7.5 and -17.8 ± 2.9 mV at pH 8.5; Fig. 2H inset). These data indicate that at least two of the tested mutants, C386R and W240S, appear to be functional but exhibit altered electrophysiological properties.

In this study, we found that five mutations R125H, W240S, C386R, V507I and N639 in human SLC4A11 altered intracellular pH homeostasis to varying degrees in transfected PS120 cells. It has been proposed that these functional differences could be due to impaired protein trafficking to the plasma membrane and in part due to a reduction in the functional electrogenic H^+ transport property of SLC4A11 mutants (Alka and Casey 2018; Vilas, Loganathan et al. 2012). We found that in the PS120 expression model, the protein amounts in the plasma membrane were not significantly different among WT and mutants, indicating that these mutations did not interfere with protein trafficking. Our data differ from a previous report proposing that C386R and W240S proteins are retained in the endoplasmic reticulum (Vilas, Loganathan et al. 2012). This discrepancy may be due to the fact that different expression models were used (transiently transfected HEK293 vs stably expressing PS120 cells in the current study) or the approach: Vilas et al. show total and unbiotinylated fractions, calculating the difference as surface expression and using GAPDH as the internal reference (Vilas, Loganathan et al. 2013), and more recently used a bioluminescence resonance energy transfer assay (Alka and Casey 2018),

while in our study we blot the biotinylated plasma membrane fraction directly with reference to Na^+/K^+ ATPase.

SLC4A11 confers NH_3-dependent H^+ fluxes (Kao, Azimov et al. 2016; Zhang, Ogando et al. 2015). We found that intracellular pH responses to NH_4Cl pulses were altered in the mutants. The intracellular rates of alkalinization/acidification are lower for all of the SLC4A11 mutants. The rate of acidification in NH_4Cl represents the NH_3 sensitive H^+ influx (Fig. 1E). The rank order of function was WT> C386R> W240S> R125H> V507I = N693A >EV. From the electrophysiological recordings, all mutants showed significantly lower NH_4Cl induced currents than WT. For patch-clamp data the rank is WT> C386R> W240S> R125H = V507I =N693A >EV, which is essentially the same as the pHi data.

Conclusion

Five SLC4A11 mutants that are associated with corneal endothelial dystrophy exhibit markedly reduced NH_3 sensitive electrogenic H^+ transport activity, with plasma membrane protein expression being unaffected in a PS120 stable transfection model. The intracellular pH rates of alkalinization/acidification in the mutants show a reduced amount of functionality when compared to the wild-type SLC4A11. Our data support the hypothesis that reduced and altered functional activity of some SLC4A11 mutants rather than membrane trafficking may underlie corneal endothelial dystrophy in patients expressing these mutations. However, there are over sixty SLC4A11 missense mutants and whether dysfunction is due to poor trafficking or activity needs further testing.

Funding Statement

This work was supported by NIH grants #R01HL115140 (AGO) and R01EY008834 (JAB).

Acknowledgements

KSH was supported by a Life-Health Sciences Internship Program at Indiana University-Purdue University Indianapolis.

ACCEPTED MANUSCRIPT

References

Alka, K. and J. R. Casey 2018. Molecular phenotype of SLC4A11 missense mutants: Setting the stage for personalized medicine in corneal dystrophies. Hum Mutat 39(5): 676-690.

Alka, K. and J. R. Casey 2018. Ophthalmic Nonsteroidal Anti-Inflammatory Drugs as a Therapy for Corneal Dystrophies Caused by SLC4A11 Mutation. Invest Ophthalmol Vis Sci 59(10): 4258-4267.

Barriere, H., C. Poujeol, M. Tauc, J. M. Blasi, L. Counillon and P. Poujeol 2001. CFTR modulates programmed cell death by decreasing intracellular pH in Chinese hamster lung fibroblasts. Am J Physiol Cell Physiol 281(3): C810-24.

Chiu, A. M., J. J. Mandziuk, S. K. Loganathan, K. Alka and J. R. Casey 2015. High Throughput Assay Identifies Glafenine as a Corrector for the Folding Defect in Corneal Dystrophy-Causing Mutants of SLC4A11. Invest Ophthalmol Vis Sci 56(13): 7739-53.

Jalimarada, S. S., D. G. Ogando, E. N. Vithana and J. A. Bonanno 2013. Ion transport function of SLC4A11 in corneal endothelium. Investigative Ophthalmology & Visual Science 54(6): 4330-40.

Kao, L., R. Azimov, N. Abuladze, D. Newman and I. Kurtz 2015. Human SLC4A11-C functions as a DIDS-stimulatable H(+)(OH(-)) permeation pathway: partial correction of R109H mutant transport. Am J Physiol Cell Physiol 308(2): C176-88.

Kao, L., R. Azimov, X. M. Shao, R. F. Frausto, N. Abuladze, D. Newman, A. J. Aldave and I. Kurtz 2016. Multifunctional Ion Transport Properties of Human SLC4A11: Comparison of the SLC4A11-B and SLC4A11-C Variants. Am J Physiol Cell Physiol: ajpcell 00233 2016.

Loganathan, S. K., H. P. Schneider, P. E. Morgan, J. W. Deitmer and J. R. Casey 2016. Functional assessment of SLC4A11, an integral membrane protein mutated in corneal dystrophies. Am J Physiol Cell Physiol 311(5): C735-C748.

Myers, E. J., A. Marshall, M. L. Jennings and M. D. Parker 2016. Mouse Slc4a11 expressed in Xenopus oocytes is an ideally selective H+/OH- conductance pathway that is stimulated by rises in intracellular and extracellular pH. Am J Physiol Cell Physiol 311(6): C945-C959.

Ogando, D. G., S. S. Jalimarada, W. Zhang, E. N. Vithana and J. A. Bonanno 2013. SLC4A11 is an EIPA-sensitive Na(+) permeable pHi regulator. American journal of physiology. Cell physiology 305(7): C716-27.

Park, M., Q. Li, N. Shcheynikov, W. Zeng and S. Muallem 2004. NaBC1 is a ubiquitous electrogenic Na+ -coupled borate transporter essential for cellular boron homeostasis and cell growth and proliferation. Molecular cell 16(3): 331-41.

Ramprasad, V. L., N. D. Ebenezer, T. Aung, R. Rajagopal, V. H. Yong, S. J. Tuft, D. Viswanathan, M. F. El-Ashry, P. Liskova, D. T. Tan, S. S. Bhattacharya, G. Kumaramanickavel and E. N. Vithana 2007. Novel SLC4A11 mutations in patients with recessive congenital hereditary endothelial dystrophy (CHED2). Mutation in brief #958. Online. Human mutation 28(5): 522-3.

Riazuddin, S. A., E. N. Vithana, L. F. Seet, Y. Liu, A. Al-Saif, L. W. Koh, Y. M. Heng, T. Aung, D. N. Meadows, A. O. Eghrari, J. D. Gottsch and N. Katsanis 2010. Missense mutations in the sodium borate cotransporter SLC4A11 cause late-onset Fuchs corneal dystrophy. Human mutation 31(11): 1261-8.

Vilas, G. L., S. K. Loganathan, J. Liu, A. K. Riau, J. D. Young, J. S. Mehta, E. N. Vithana and J. R. Casey 2013. Transmembrane water-flux through SLC4A11: a route defective in genetic corneal diseases. Hum Mol Genet 22(22): 4579-90.

Vilas, G. L., S. K. Loganathan, A. Quon, P. Sundaresan, E. N. Vithana and J. Casey 2012. Oligomerization of SLC4A11 protein and the severity of FECD and CHED2 corneal dystrophies caused by SLC4A11 mutations. Hum Mutat 33(2): 419-28.

Vithana, E. N., P. Morgan, P. Sundaresan, N. D. Ebenezer, D. T. Tan, M. D. Mohamed, S. Anand, K. O. Khine, D. Venkataraman, V. H. Yong, M. Salto-Tellez, A. Venkatraman, K. Guo, B. Hemadevi, M. Srinivasan, V. Prajna, M. Khine, J. R. Casey, C. F. Inglehearn and T. Aung 2006. Mutations in sodium-borate cotransporter SLC4A11 cause recessive congenital hereditary endothelial dystrophy (CHED2). Nat Genet 38(7): 755-7.

ACCEPTED MANUSCRIPT

Vithana, E. N., P. E. Morgan, V. Ramprasad, D. T. Tan, V. H. Yong, D. Venkataraman, A. Venkatraman, G. H. Yam, S. Nagasamy, R. W. Law, R. Rajagopal, C. P. Pang, G. Kumaramanickevel, J. R. Casey and T. Aung 2008. SLC4A11 mutations in Fuchs endothelial corneal dystrophy. Hum Mol Genet 17(5): 656-66.

Zhang, W., D. G. Ogando, J. A. Bonanno and A. G. Obukhov 2015. Human SLC4A11 Is a Novel NH3/H+ Co-transporter. J Biol Chem 290(27): 16894-905.

Table 1. PCR primers used for *SLC4A11* Mutagenesis.

Mutation	Primers (5' -> 3')
R125H	Forward: AACTTCAAGGAAGAGATCCATGCGCACCGCGACCTAGAT Reverse: ATCTAGGTCGCGGTGCGCATGGATCTCTTCCTTGAAGTT
W240S	Forward: CACAGAACTCGGGGGAGAATTCCTGTGAGGTTC Reverse: GAACCTCACAGGAATTCTCCCCCGAGTTCTGTG
C386R	Forward: CTGTTCCTCTACTTCGCCCGCCTCCTG Reverse: CAGGAGGCGGGCGAAGTAGAGGAACAG
V507I	Forward: CATCACGTTTGTGCTGGATGCCATCAAGGGCAC Reverse: GTGCCCTTGATGGCATCCAGCACAAACGTGATG
N639A	Forward: GATGAGCAAGTTCCGCTACGCCCCCAGCGAGAG Reverse: CTCTCGCTGGGGGCGTAGCGGAACTTGCTCATC

Mutated nucleotides were indicated by underline.

ACCEPTED MANUSCRIPT

ACCEPTED MANUSCRIPT

Table 2. SLC4A11 and mutants current densities (a-e are indicated in Fig. 2).

		Current Densities (pA/pF)	P (vs WT)	P (vs EV)
WT (n=17)	a	-6.42 ± 1.67	N.C.	P<0.05
	b	1.04 ± 0.36	N.C.	N.S.
	c	-22.09 ± 2.24	N.C.	P<0.001
	d	-1.92 ± 0.61	N.C.	N.S
	e	-4.60 ± 0.50	N.C.	P<0.05
C386R (n=8)	a	-0.97 ± 0.51	P<0.05	P<0.05
	b	-0.38 ± 0.30	P<0.05	N.S.
	c	-3.00 ± 0.63	P<0.001	P<0.05
	d	-3.93 ± 0.97	P<0.05	P<0.05
	e	-4.05 ± 0.99	N.S	P<0.05
W240S (n=8)	a	-0.56 ± 0.28	P<0.05	N.S.
	b	-0.30 ± 0.19	P<0.05	N.S.
	c	-1.64 ± 0.24	P<0.001	P<0.05
	d	-1.28 ± 0.29	N.S.	N.S.
	e	-1.23 ± 0.32	P<0.05	P<0.05
R125H (n=6)	a	0.12 ± 0.19	P<0.05	N.S.
	b	-0.62 ± 0.45	N.S.	N.S.
	c	-0.66 ± 0.11	P<0.001	N.S.
V507I (n=6)	c	-0.74 ± 0.24	P<0.001	N.S.
N693A (n=5)	a	0.91 ± 0.26	P<0.05	N.S.
	b	-0.29 ± 0.09	N.S.	N.S.
	c	-0.60 ± 0.19	P<0.001	N.S.
EV (n=6)	a	-0.19 ± 0.10	P<0.05	N.C.
	b	-0.11 ± 0.05	N.S.	N.C.
	c	-0.58 ± 0.06	P<0.001	N.C.
	d	-1.14 ± 0.28	N.S	N.C.
	e	-1.34 ± 0.36	P<0.05	N.C.

N.C. stands for not compared; N.S. stands for no significant difference. Each individual measurement was taken from one individual cell per coverslip. “n” represents the number of tested individual cells.

ACCEPTED MANUSCRIPT

Figure 1.

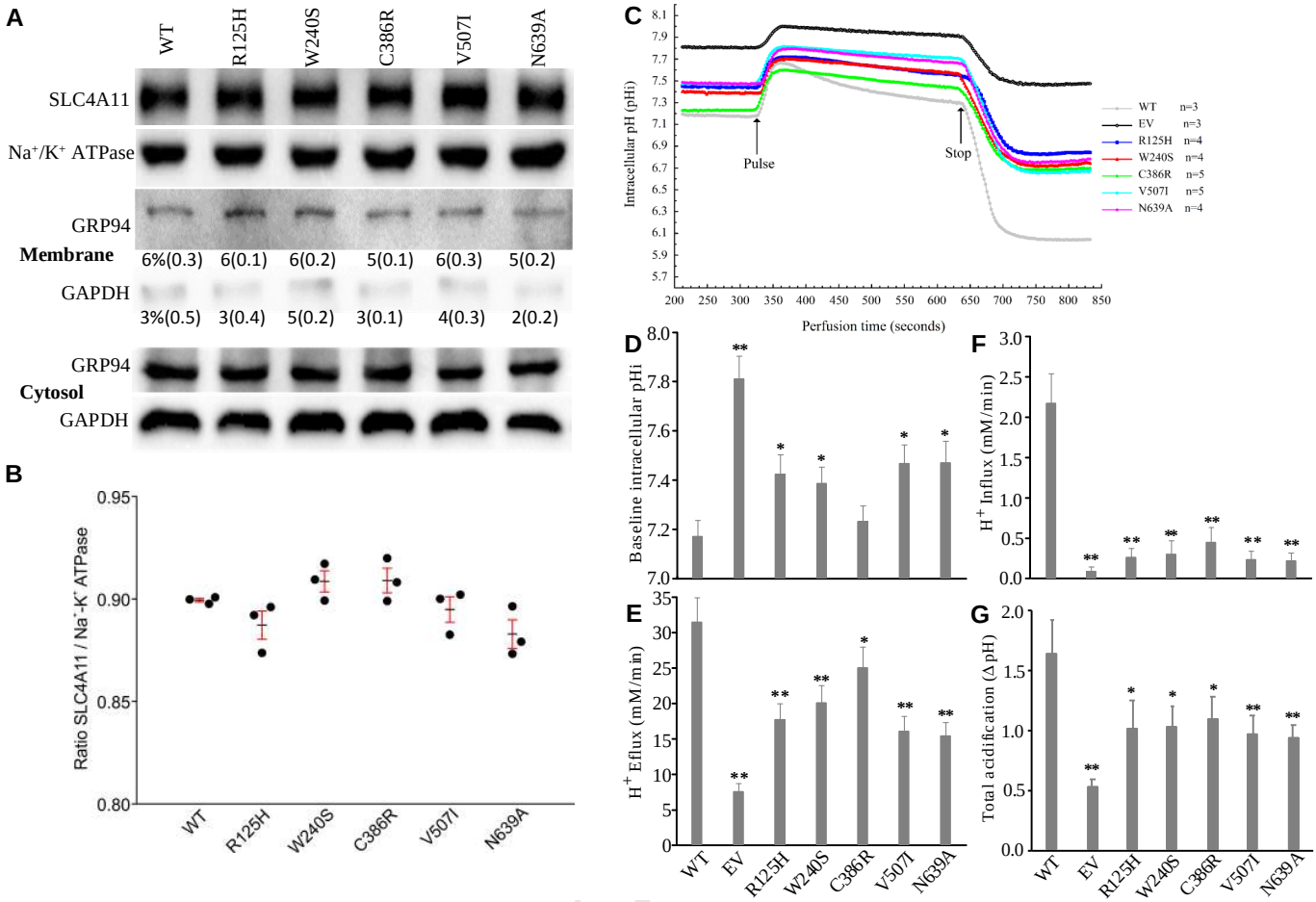

Fig. 1. SLC4A11 expression in plasma membrane and H^+ Flux. (A) Shows a representative western blot image of biotinylated SLC4A11 and (Na^+/K^+)-ATPase, selected from three independent experiments (n = 3). Procedure validation was performed by probing biotinylated and non-biotinylated fractions for GRP94, an ER resident protein, and cytosolic GAPDH. Percent in membrane fraction and (SD) are shown. (B) Plot of SLC4A11/(Na^+/K^+)-ATPase ratio for WT and each mutant showing the individual ratios from each experiment, the mean and SD, p>0.05. (C) The measurement of intracellular pH in PS120 cells. Average pHi traces from three or more independent experiments as indicated. Pulse with 10 mM NH_4Cl was maintained for 300 seconds. (D) Baseline pHi. (E) H^+ efflux during initial 10 seconds of NH_4Cl pulse. (F) H^+ influx in the presence of NH_4Cl (between Pulse and Stop). (G) Total acidification which is the difference between baseline pHi and lowest pHi after removing NH_4Cl. The values represent the average in n=3 tests and are shown as mean±SD. One-way ANOVA test in a comparison to WT, * indicates $p < 0.05$ and ** indicates $p < 0.01$.

ACCEPTED

Figure 2.

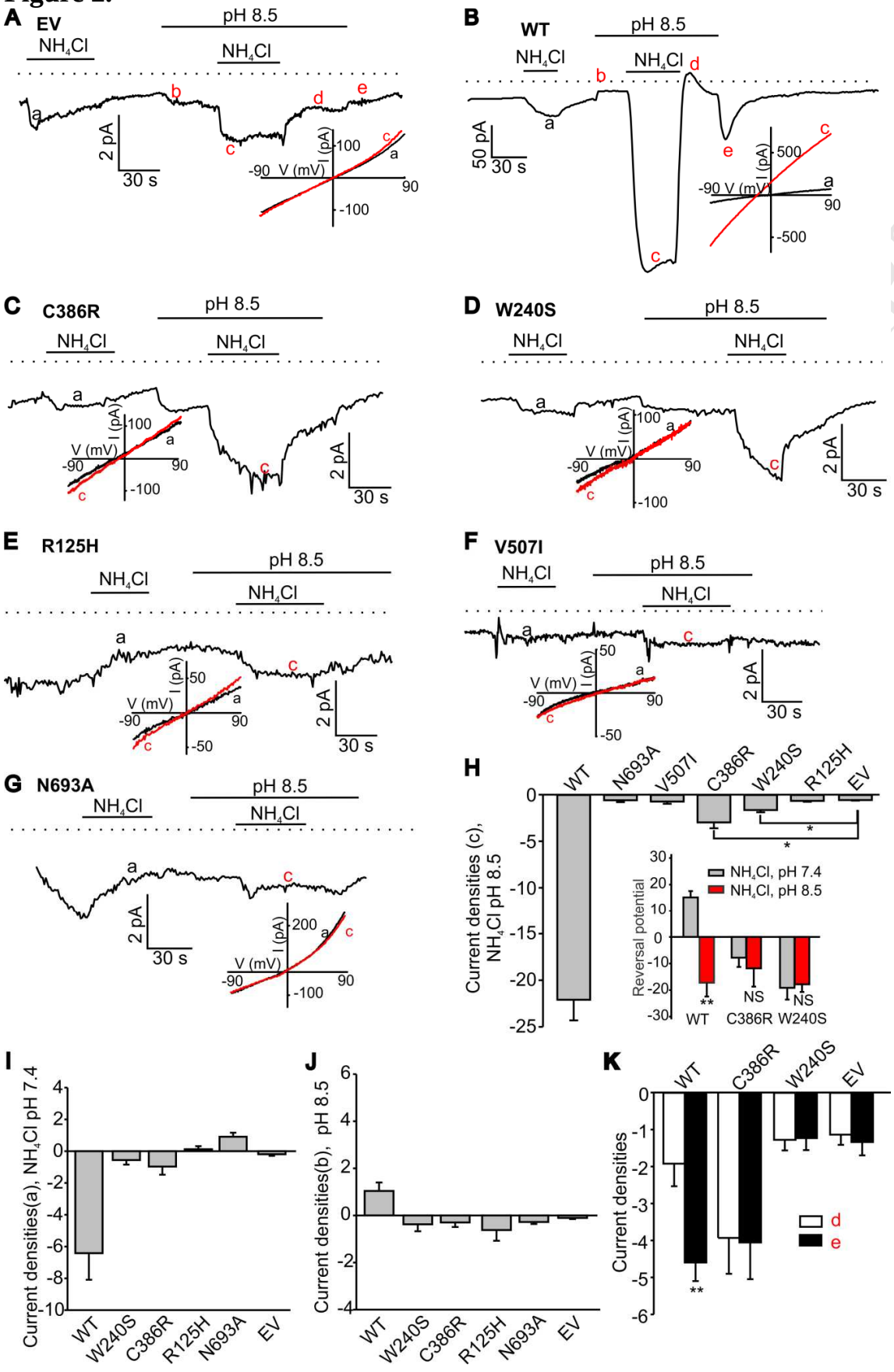
A EV
pH 8.5
NH4Cl
NH4Cl
2 pA
30 s
I (pA)
V (mV)
B WT
50 pA
C C386R
D W240S
E R125H
F V507I
G N693A
H
WT
N693A
V507I
C386R
W240S
R125H
EV
Current densities (c), NH4Cl pH 8.5
NH4Cl, pH 7.4
NH4Cl, pH 8.5
Reversal potential
NS
I
Current densities(a), NH4Cl pH 7.4
J
Current densities(b), pH 8.5
K
Current densities
d
e

ACCEPTED MANUSCRIPT

Figure 2. Ammonia-induced inward currents in PS120 cells expressing SLC4A11 or its indicated mutants.

A. A sample control trace from an empty vector (EV) expressing PS120 cell. **(B-G)** Sample traces of NH_4Cl-induced currents observed in PS 120 cells expressing WT-SLC4A11 or mutants. The horizontal lines indicate the times when solution pH level was altered and/or NH_4Cl was added. The dotted lines show the zero current level. Alkalinization of extracellular solution to pH 8.5 induced small inward currents before the second NH_4Cl pulse in both C386R and W240S mutants. The insets in (A-G) show the current-voltage curves for each trace recordings obtained at different pH values. The Summary data of pH 8.5-NH_4Cl and pH 7.4-NH_4Cl induced current densities are shown in (H) and (I). The inset in (H) shows the reversal potential of pH 8.5-NH4Cl and pH 7.4-NH4Cl induced WT, C386R and W240S currents (J) shows the current densities induced by pH 8.5 solution alone. The peak values at the points when the solution changes from pH 8.5-NH_4Cl to pH 8.5 (d point in red) and from pH 8.5 to pH 7.4 (e point in red) are shown in (H). The significantly different groups are indicated with asterisks. The statistical analysis is included in Table 2. (K) changes in the current flow direction upon re-addition of pH 7.5 solution after an NH_4Cl extracellular pulse (see points d and e in figure 2B). **, $p<0.01$. NS stands for "not significant."

ACCEPTED MANUSCRIPT